Dig Dis Sci (2013) 58:2528–2541
DOI 10.1007/s10620-013-2755-1

ORIGINAL ARTICLE

Mucosal Addressin Cell Adhesion Molecule (MAdCAM-1) Expression Is Upregulated in the Cirrhotic Liver and Immunolocalises to the Peribiliary Plexus and Lymphoid Aggregates

Aftab Ala · David Brown · Korsa Khan · Richard Standish · Joseph A. Odin · M. Isabel Fiel · Thomas D. Schiano · Kenneth J. Hillan · Syed A. Rahman · Humphrey J. F. Hodgson · Amar P. Dhillon

Received: 23 June 2012 / Accepted: 12 June 2013 / Published online: 10 July 2013

Abstract
Background Enhanced cell expression of MAdCAM-1 is critical in tissue recruitment of lymphocytes in response to stimuli expressing the $\alpha 4\beta 7$ integrin. MAdCAM-1 is well characterized in gut mucosa with emerging evidence of hepatic expression.
Aims (i) Compare quantitative/semi-quantitatively MAdCAM-1 expression in relation to early and advanced liver diseases (ii) Define the fine structure of vascular plexuses/lymphatics in the portal tract on which MAdCAM-1 is expressed.
Methods Using alkaline phosphatase anti-alkaline phosphatase methodology on paraffin embedded tissue sections ($n = 28$) from cirrhotic individuals who underwent orthotopic liver transplant, we evaluated MAdCAM-1 expression and compared with pre-cirrhotic, fulminant hepatitis B, and non-cirrhotic portal hypertension tissue sections. The positive controls included normal colon tissue with negative controls without primary antibody and isotype-matched purified IgG. We developed a real time PCR to quantify levels of MAdCAM-1 mRNA in our samples.
Results MAdCAM-1 was expressed in 27/28 of the cirrhotic sections, localized primarily to septal areas within (i) endothelium of the peribiliary vascular plexus (PBP) (ii) lymphoid aggregates, with absence from normal, non-cirrhotic portal hypertension and pre-cirrhotic livers. There was significant upregulation of MAdCAM-1 mRNA in cirrhosis ($p < 0.011$), consistent with immunohistochemical analysis.

A. Ala
Faculty of Health & Medical Sciences and Faculty of Health Care Management & Policy, University of Surrey, Surrey GU2 7TE, UK

A. Ala (✉)
Centre for Gastroenterology, Hepatology and Nutrition, Frimley Park Hospital NHS Foundation Trust, Surrey GU16 7UJ, UK
e-mail: aftab.ala@fph-tr.nhs.uk

D. Brown · H. J. F. Hodgson
Institute for Liver & Digestive Health, UCL Medical School, Royal Free Campus, London NW3 2PF, UK

K. Khan · R. Standish · A. P. Dhillon
Department of Cellular Pathology, UCL Medical School, Royal Free Campus, London NW3 2PF, UK

J. A. Odin · T. D. Schiano
Division of Liver Diseases, Department of Medicine and Recanti/Miller Transplantation Institute, Icahn School of Medicine at Mount Sinai, Madison Avenue, New York, NY, USA

M. I. Fiel
Henry M. Stratton-Hans Popper Department of Pathology, Icahn School of Medicine at Mount Sinai, Madison Avenue, New York, NY, USA

K. J. Hillan
Institute of Pathology, GeneTech, South San Francisco, San Francisco, CA, USA

S. A. Rahman
European Molecular Biology Laboratory-European Bioinformatics Institute, Wellcome Trust Genome Campus, Hinxton, UK

Conclusions MAdCAM-1 is up-regulated in cirrhosis with expression on PBP and lymphoid aggregates. MAdCAM-1 is likely to contribute to the localization and recruitment of α4β7 lymphocytes during the pathogenesis of cirrhosis. MAdCAM-1 could be a useful marker of advanced liver disease. Further studies with respect to the expression of MAdCAM-1 in the presence of reversible and non-reversible stages of liver disease may be of merit.

Keywords MAdCAM-1 · Adhesion molecule · Cirrhosis · Peribiliary plexus · Lymphoid aggregate · Chronic liver disease

Introduction

Recruitment of leukocytes from the circulation is a pivotal step in inflammation. The ligand-receptor interactions mediating the emigration of specific cell-types into individual organs affected by inflammation are crucial to our understanding of gastrointestinal disease [1]. Such interactions are important as they have the potential ability to act as targets for therapeutic gain. One such important target in the gut is the interaction between mucosal addressin cell adhesion molecule (MAdCAM-1) and its ligand, the lymphocyte integrin α4β7 [2, 3].

MAdCAM-1 was first recognised on murine endothelial cells in the gut lamina propria, mesenteric nodes, mammary gland, and on follicular dendritic cells (FDC) of mucosal lymphoid organs (Peyer's patches) but not peripheral lymph nodes [4–7]. The expression of MAdCAM-1 in experimental gut inflammation increases and α4β7 is therefore decisively placed to mediate the homing of these lymphocytes to mucosal organs [8–10].

Enhanced cell expression of MAdCAM-1 is important in tissue recruitment of lymphocytes in response to a variety of stimuli expressing the α4β7 cell surface integrin. In addition to its well-characterized expression and role in the gastrointestinal tract mucosa, where MAdCAM-1 regulates lymphocyte trafficking, there is emerging evidence of its hepatic expression in those with liver disease, e.g. primary sclerosing cholangitis (PSC), but its specific participation in the pathogenesis of liver disease is currently undefined [11, 12].

In chronic liver diseases, persistently increased hepatic inflammation is believed to lead to increasing fibrosis and eventually cirrhosis, end stage liver disease. Our hypothesis is that inflammatory processes within the liver progressively induce local upregulation of MAdCAM-1 expression. That is, the regional vascular distribution of MAdCAM-1 upregulation is related to the degree and distribution of inflammation within the liver lobule and portal tracts. Our aims of the study were to (1) compare semi-quantitatively the expression of MAdCAM-1 in early and advanced liver disease, (2) define the fine structure of vascular plexuses, lymphatics in the portal tract, particularly the peribiliary vascular plexus (PBP), bile ducts on which MAdCAM-1 may be expressed, and (3) determine the presence and distribution of MAdCAM-1 in immune and non-immune mediated liver disease, with and without co-existing gut inflammation. The ability to detect the presence of MAdCAM-1 and ultimately quantify its expression could be potentially useful in the diagnosis and subsequent management of chronic inflammatory and immune mediated diseases affecting the liver.

Methods

MAdCAM-1 expression was determined by immunohistochemistry on human liver from a total of 28 patients with cirrhosis who underwent orthotopic liver transplant (OLT). Pre-cirrhotic liver tissues were taken from needle biopsy specimens of PBC stages 1–2 (5 females), PSC stages 1–2 (3 males), HCV stages 1–2 (3 males, 2 females), and explants from hepatitis B fulminant liver failure (2 males). Normal liver tissues were obtained from three liver biopsies, four partial hepatectomies performed for colorectal metastasis with wide resection margins and four sections of extra hepatic biliary obstruction obtained from trucut liver biopsies during staging laparoscopy for pancreatic adenocarcinoma. There were three liver biopsies from chronic rejection after OLT. There were two specimens of non-cirrhotic portal hypertension obtained from transjugular liver biopsies. The positive controls for MAdCAM-1 expression were taken from samples of normal explant colon tissue.

The diagnoses of PBC, PSC, ALD, HCV, HBV and chronic ductopenic rejection were made on established criteria [13].

All tissues were fixed in 10 % buffered formalin and embedded in paraffin. Four micron sections were cut on to APES (3-aminopropyltriethoxysilane) coated slides, one section being stained with haematoxylin and eosin. A three-stage immuno-alkaline phosphatase (APAAP) technique was applied.

Alkaline Phosphatase Anti-Alkaline Phosphatase (APAAP) Methodology

Sections were deparaffinised in xylene, dehydrated in alcohol, re-hydrated in water, and immersed in 15 % acetic acid for 20 min to block endogenous alkaline phosphatase. They were then treated with 1 mmol/l EDTA (pH 8) in a pressure cooker followed by cooling. After rinsing in TRIS buffered saline (TBS) pH 7.6, slides were incubated in

10 % normal goat serum (Dako) for 20 min followed by polyclonal rabbit anti-human MAdCAM-1 (2 μg/ml, a gift from Genetech, San Francisco, USA) overnight at 4 °C. Sections were then thoroughly washed in TBS, and incubated with alkaline phosphatase conjugated goat anti-rabbit IgG antibody (1:50 Sigma Aldrich, Poole, UK) for 1 h at room temperature. The sections were washed with TBS again and incubated with fast red substrate (diazotised 5-nitroanisidine 1-5-naphthalene disulphonate, Dako, UK) for 30 min, followed by brief counter staining with Mayer's hematoxylin (Sigma Aldrich, Poole, UK). The slides were mounted in DPX (ProSciTech) and observed using light microscopy.

Dendritic Cell and Lymphatic Vessel Staining

A panel of adjacent serial sections from tissue were also immunostained for a subset of dendritic cells, including CD21, CD68 and S100 to elucidate the site of the MAdCAM-1 immunoreactivity in the lymphoid aggregates using the APAAP methodology as described above.

Monoclonal antibodies to CD21 were used to identify FDC, CD68 to recognise monocyte/macrophage and dendritic cell, and S100 to antigen presenting cells such as interdigitating dendritic cells. Sections were incubated with primary antibody for 1 h. Blocking was performed with normal goat serum (1:10, DAKO UK Ltd) followed by incubation with rabbit anti-mouse antibody (1:25, DAKO UK Ltd) and then with alkaline phosphatase-conjugated mouse anti-alkaline phosphatase (1:50, DAKO UK Ltd).

Some sections were stained to demonstrate lymphatic endothelium using anti-podoplanin antibody. Microwave pre-treatment was followed by labeling with rabbit anti-human podoplanin IgG for 60 min at room temperature and washing in PBS then incubated with biotinylated goat anti-rabbit antibodies (Vector). The staining was visualized using a streptavidin–peroxidase complex (Vector), diamino-benzidine and H_2O_2. Sections incubated without primary antibodies were used as negative controls.

Immunofluorescence Microscopy

After pre-treatment, sections were incubated with anti-human MAdCAM-1 (1:150) and antiCD34 (1:100) primary antibodies. They were then washed in PBS and incubated with secondary antibody (goat anti-rabbit FITC and goat anti-mouse Texas Red, both 1:50 in PBS) for 1 h at room temperature. Images were acquired with a Zeiss Axiophot fluorescence microscope using an Axiocam HRc camera and further processed using AxioVision 4.5 software (Carl Zeiss; Fig. 3).

Representative sections were incubated with anti-CD21 (1:100), anti-CD68 (1:50), anti-S100 (1:50) and anti-human MAdCAM-1 (1:150) primary antibodies. They were subsequently washed in PBS and incubated with secondary antibody (goat ant-rabbit FITC and goat anti-mouse Texas Red, both 1:50 in PBS) for 1 h at room temperature and examined by fluorescence microscopy (Fig. 3).

Immunohistochemical Assessment

Two observers (AA and RS) independently assessed the sections semi-quantitatively and scored the staining on a scale of 0 to +3 according to the intensity and distribution of MAdCAM-1 immunoreactivity (0, no staining; +1, mild and focal staining identified at higher magnification 40× after scrupulous searching; +2, moderate patchy staining identified at low magnification; and +3, marked strong diffuse staining identified at lower magnification). The staining methods were repeated twice to validate the scoring system. There was 100 % interobserver variability. Particular attention was paid to areas of lymphoid aggregation and vascular endothelium, specifically in the vessels of the PBP. The sections were also examined for staining of hepatocytes, biliary epithelium and sinusoid lining cells. The bile ducts were analyzed in three categories according to size: proliferating bile ductules (the smallest duct branches with a generally inconspicuous lumen, usually confined to marginal zones in portal areas), interlobular ducts (small ducts, diameter 20–100 μm), and large ducts of greater than 100 μm in diameter, usually septal or trabecular ducts. Negative controls incubated without primary antibody or with isotype-matched anti-IgG were included in all experiments.

Development of a Reverse Transcriptase-Polymerase Chain Reaction (RT-PCR) Assay to Assess MAdCAM-1 Expression in Control Colon Tissues

Primer pairs designed using the online program (http://frodo.wi.mit.edu/) were used including forward 5′-CGGGC CGCAGCGTCCTCAC-3′ and reverse 5′-TCCCCCTGTG AAAGCAAAAT-3′. A 100-μg fresh tissue sample of histologically normal colon tissue as positive control was snap frozen in liquid nitrogen and cryopreserved at −80 °C until RNA extraction. TRIzol^{R} Reagent (Invitrogen) was used for isolation of total RNA following manufacturer's instructions.

Reverse Transcription/PCR

Ten pmol of oligo dT primer was added to 20 μl of RNA (DNase treated) and incubated at 65 °C for 5 min. This was then added to the reverse transcription mix as detailed below and incubated at 37 °C for 60 min. The reaction was

terminated by heating to 70 °C for 15 min and the cDNA stored at 20 °C until use. The cDNA was then amplified by single round PCR using the hot start Taq DNA polymerase kit (Hotstar, Qiagen, UK) to minimize amplification of non-specific product. The PCR consisted of 15 min incubation at 95 °C to activate the Taq polymerase, followed by 35 cycles each consisting of denaturation at 94 °C for 30 s, primer annealing at 60 °C for 30 s and extension at 72 °C for 1 min.

Gel Electrophoresis, Extraction of PCR DNA

Analysis of the PCR product was carried out by agarose gel electrophoresis. The DNA amplicon was extracted from the agarose gel using QIAquick Gel Extraction Kit (QIAGEN, UK). The DNA fragment was excised from the agarose gel and three volumes of Buffer QG were added to one volume of gel. This was incubated at 50 °C for 10 min until the gel slice had completely dissolved. To increase the yield of DNA fragments one volume of isopropanol was added and mixed thoroughly. The mixture was loaded onto a QIAquick spin column and centrifuged for 1 min at 13,000 rpm. The flow-through was discarded and a further 0.5 ml of Buffer QG Buffer was added and centrifuged for a further 1 min to remove all traces of agarose. Buffer PE (0.75 ml) was added to the column and centrifuged again for 1 min at 13,000 rpm. The flow-through was discarded and the column centrifuged for an additional 1 min at 13,000 rpm to ensure complete removal of wash buffer. The column was placed into a clean 1.5 ml-microcentrifuge tube and the DNA eluted with 30 µl 10 mM Tris pH 7.4. The DNA was stored at −20 °C until used.

DNA Sequencing

The amplicon was directly sequenced using forward and reverse primers by The Sequencing Service (School of Life Sciences, University of Dundee, Scotland, www.dnaseq.co.uk) using Applied Biosystems Big Dye Ver 3.1 chemistry and an Applied Biosystems 3730 automated capillary sequencer.

Development and Use of a Real-Time PCR Assay to Quantify MAdCAM-1 mRNA in Human Disease

Isolation of Total RNA from Human Tissue

Fresh diseased and normal liver tissues ($n = 14$: 4 normal, 3 PBC cirrhosis, 3 PSC cirrhosis, 4 ALD cirrhosis) were cut into small pieces (50–100 mg), snap frozen in liquid nitrogen immediately after removal and stored at −80 °C until use. Total RNA was isolated using the Qiagen RNeasy Mini Kit (QIAGEN Ltd, Crawley, UK) and stored at −80 °C until use.

Quantitative RT-Polymerase Chain Reaction

cDNA was prepared using the Sensiscript Reverse Transcription kit (Qiagen Ltd, Crawley, UK). Ten microlitres (approximately 50 ng) of RNA was added to a 10 µl reaction mix containing 1× RT buffer, 0.5 mM dNTPs, 1 µM random hexamer primers, 1U RNase inhibitor and 1 µl Sensiscript reverse transcriptase. The reaction was incubated at 37 °C for 60 min and finally heated at 95 °C for 5 min to inactivate the enzyme. cDNA was stored at −20 °C until use.

Primers MAdCAM-1 designed as described for qualitative PCR were used for real-time quantitation of MAdCAM-1 mRNA utilizing Sybr Green reagents. A standard curve was included in each run comprising DNA copies of the PCR product in the range 10^3–10^8 per reaction. Reaction conditions were: 5 µl cDNA, 1× buffer, 5 mM $MgCl_2$, 0.2 mM dNTPs, 1 µM each Primer F5 and R6, Sybr Green (1/75,000), and 1U Platinum Taq DNA polymerase (Invitrogen) in a final volume of 25 µl. Thermal cycling and data acquisition was carried out on a Rotor-Gene RG-3000 (Corbett Research, Mortlake, Australia) using the following conditions: 95 °C for 15 min; 44 cycles of 94 °C for 30 s, 60 °C for 30 s, 72 °C for 60 s and a melt curve between 50 and 99 °C. All samples were measured in duplicate. Standard curves were constructed by regression analysis and unknowns calculated using Rotor-Gene software.

Sample copy numbers were normalized for 18S RNA by carrying out real-time RT-PCR on each sample as described using 18S RNA primers (sense, 5′-GTATTGCGC CGCTAGAGGTG; anti-sense, 5′-CTGAACGCCACTTGT CCCTC) and comparative amounts calculated against a standard RNA included in each run. Normalized copies were calculated by dividing measured values by comparative 18S RNA value.

Duplicate samples on serial dilutions of standard MAdCAM-1 cDNA were used to establish the reproducibility and accuracy of the assay. The assay for the standard 18 s internal controls had previously been verified by Oswell, Southampton, UK. We tested standard concentrations of 18S RNA in number of PCR reactions provided by the manufacturer to verify the accuracy of the 18S internal controls prior to testing our samples. To establish the accuracy of this real-time PCR protocol in quantifying MAdCAM-1DNA we used the biogene software to generate a standard curve for serial dilutions.

Statistical Analysis

The statistical differences were determined using a two-way analysis of variance (ANOVA) with significance accepted as $p < 0.05$. The results were represented as median SD of the real-time data.

Results

Characteristics of Patients

The following groups of patients (total $n = 28$) with cirrhosis who underwent OLT and from whose explants were studied: PSC, $n = 9$ (5 male, 4 female, age range 22–57, median 53 years); PBC, $n = 7$ (all females, age range 36–51, median 50 years); ALD, $n = 7$ (5 males, 2 females age range 33–64 years, median 48 years); and HCV, $n = 5$ (all males, age range 44–57, median 51 years).

Positive and Negative Controls

Positive controls taken from sections of normal colonic tissue (Fig. 1) demonstrated expression of MAdCAM-1 on vascular endothelium within the lamina propria and submucosa. Negative controls included without primary antibody or with isotype matched antiIg showed absence of MAdCAM-1, as was the case in chronic rejection, acute HBV liver failure and non-cirrhotic portal hypertension.

MAdCAM-1 Is Not Expressed in Normal and Pre-cirrhotic Liver but Expressed in Cirrhotic Liver

MAdCAM-1 immunoreactivity was present in the majority of cirrhotic sections (27/28 of explant liver tissue). Its expression was localized primarily to septal areas mainly within the (1) endothelium of the PBP and (2) lymphoid aggregates. Early stage specimens (i.e. pre-cirrhotic) in PBC, PSC, HCV, and acute fulminant hepatitis B were studied to characterize the time course of MAdCAM-1 and assess its expression in relation to the degree of inflammation and bile duct loss. It failed to show expression of MAdCAM-1. Only one patient with PSC cirrhosis had weak staining of two small vessels at the edge of parenchymal nodules. There was no evidence of expression in hepatocytes, biliary epithelium, hepatic artery, septal connective tissue or sinusoids from any of the liver sections.

MAdCAM-1 Is Expressed on the PBP in Cirrhosis

Around the large to medium bile ducts, there were distinct vessels which showed MAdCAM-1 immunoreactivity representing the PBP (Fig. 2). In PSC, the majority of sections (7/9) showed MAdCAM-1 expression in PBP vessels around large to medium sized bile ducts. Overall, moderate patchy staining in the PBP appeared to be more frequently present around ducts in PSC, compared to the other disease states, over the end-stage cirrhotic samples from other disease, e.g. PBC, ALD, HCV. Double staining with anti-MAdCAM-1 and anti-CD34 demonstrated co-localisation of CD34 and MAdCAM-1 in structures resembling PBP capillaries (Fig. 3a–c; Table 1).

MAdCAM-1 Is Expressed in Lymphoid Aggregates in Cirrhosis (Figs. 2, 3)

Most patients expressed MAdCAM-1 within septal lymphoid aggregates (6/9 PSC, all PBC, and HCV cases). This

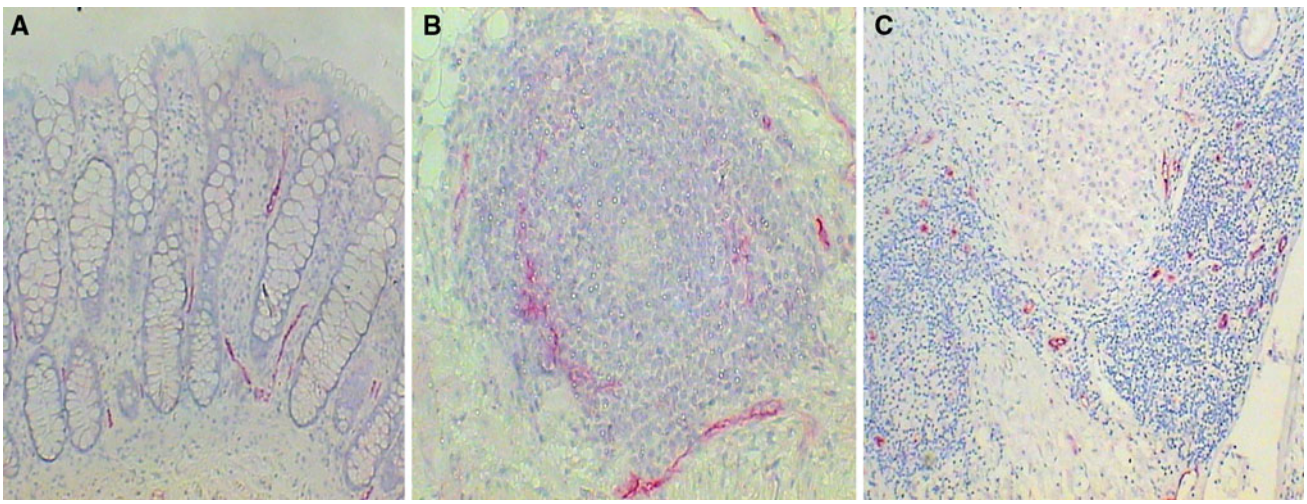

Fig. 1 MAdCAM-1 immunoreactivity patterns in vessels and lymphoid aggregates from normal colon (**a**–**b**) and cirrhotic liver (**c**). MAdCAM-1 immunoreactivity (*red*) in formalin fixed tissue sections of vascular endothelium from colon explants of histologically normal large bowel tissue (i and ii), where MAdCAM-1 is localised to endothelial lined venules of the lamina propria and submucosa (iii) gut associated lymphoid tissue, with differential expression of MAdCAM-1 in venules within lymphoid aggregates of the submucosa, compared to sub-serosa

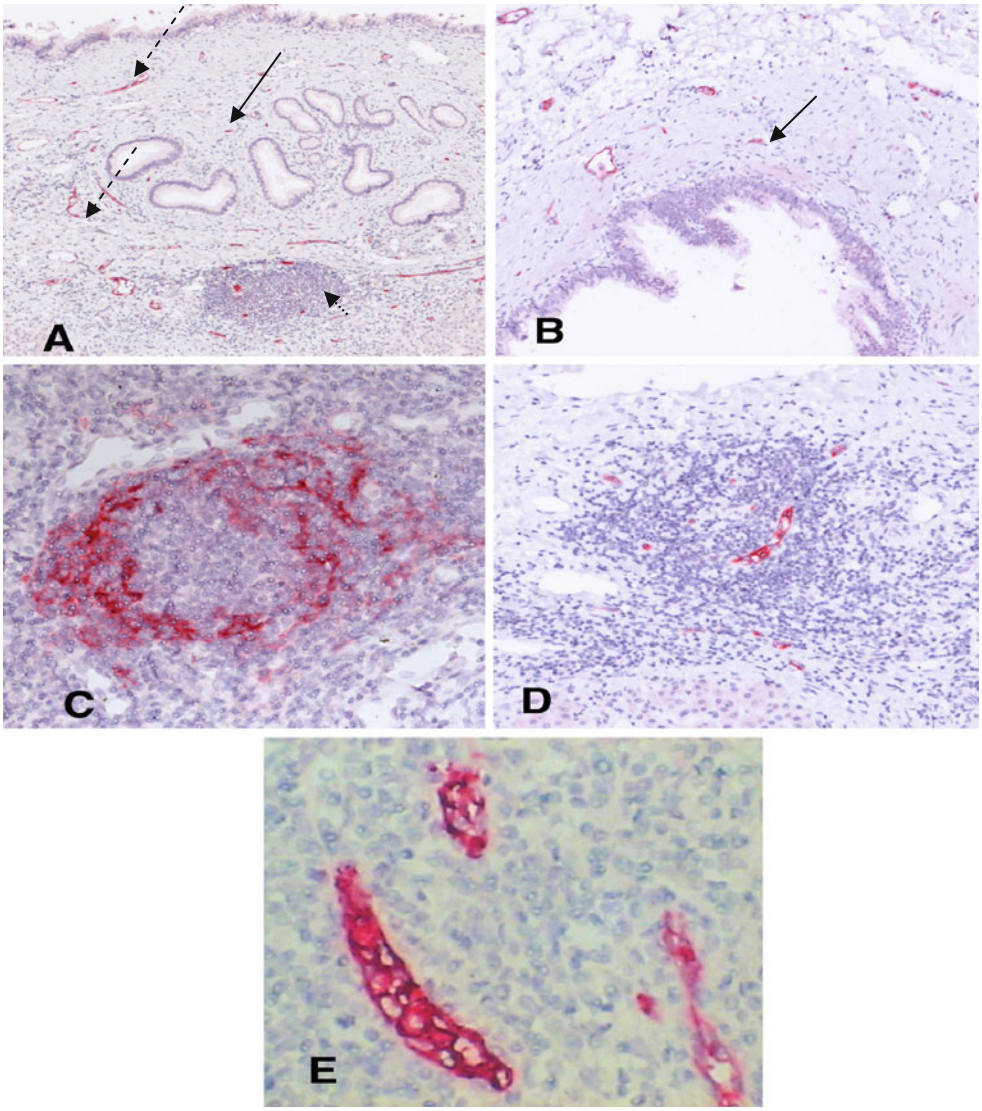

Fig. 2 **a–e** MAdCAM-1 immunoreactivity patterns in vessels and lymphoid aggregates from cirrhotic liver explants of PSC and PBC. **a** and **b** show MAdCAM-1 immunostaining of vessels around peribiliary glands, adjacent to a lymphoid aggregate (*arrow head*). These vessels represent the (*continuous and broken arrow*) peribiliary plexus (plate **b** higher magnification ×10 objective). The pattern of staining of the lymphoid aggregate (plate **c**) appears to correspond to FDC. The lymphoid aggregates have two main MAdCAM-1 immunoreactivity patterns: "peripheral" (plate **c**) and "central" (plate **d**). The high endothelial venules are MAdCAM-1 immunoreactive vessels (plate **e**) within lymphoid aggregates which are likely to represent areas of lymphocyte egress. (Alkaline phosphatase/fast red immunostaining: magnification ×5 objective **a**; ×10 objective **b**, **c** and **d**; ×20 objective **e**). **f–k** MAdCAM-1 immunoreactivity patterns in vessels and lymphoid aggregates from cirrhotic liver explants of HCV and ALD. **f** and **j** demonstrate MAdCAM-1 staining in lymphoid aggregate, showing "peripheral" and "central" patterns respectively in HCV. **h** and **i** are immunoreactive vessels from around and in HCV lymphoid aggregates. **j** and **k** demonstrate immunoreactivity of vessels around the medium-sized peribiliary glands in ALD. There is the distinct lack of lymphoid aggregates in ALD. (Alkaline phosphatase/fast red immunostaining: magnification ×5 objective **h** and **j**; ×10 objective **k**; ×20 objective **f**, **j**, **i**)

appeared as two distinct forms: (1) away from the aggregate centre in a "peripheral" pattern (3/9 PSC and 6/7 PBC) or (2) in vessel endothelium—"central" pattern of MAdCAM-1 staining (6/7 PSC and 3/9 PBC). Four of seven had moderate to marked MAdCAM-1 staining intensity conforming to the "peripheral" pattern compared to only two of seven in a central pattern of similar intensity. Most of the PSC cases had light and focal MAdCAM-1 immunoreactivity (5/9) and only one had moderate and patchy staining to MAdCAM-1. The patients with HCV had similar peripheral (5/5)/central staining and intensity (4/5) patterns.

The immunoreactivity staining patterns of MAdCAM-1 within lymphoid aggregates from PBC were noteworthy compared to PSC and HCV. There was absence of lymphoid aggregates in ALD. From the results, it appears that

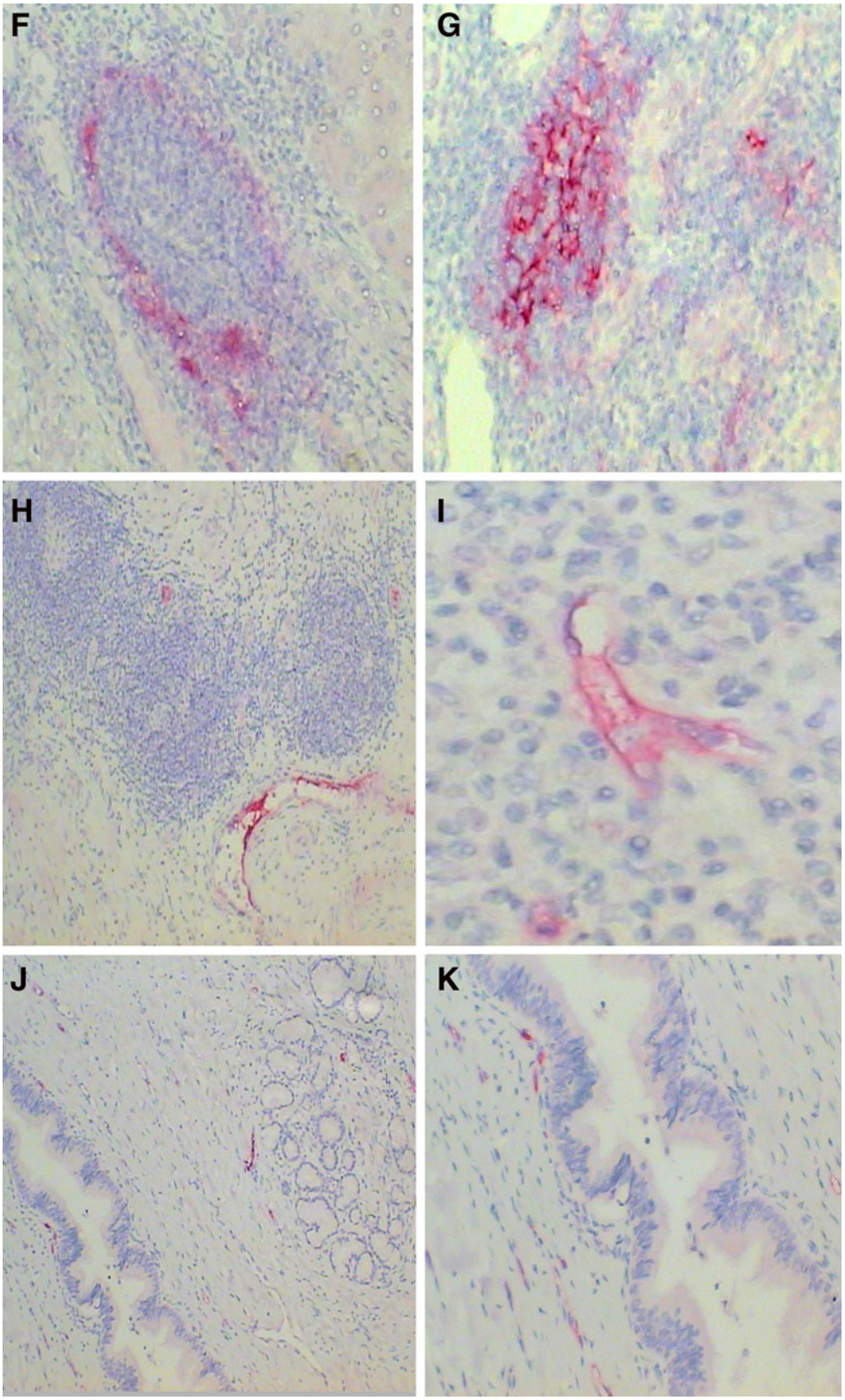

Fig. 2 continued

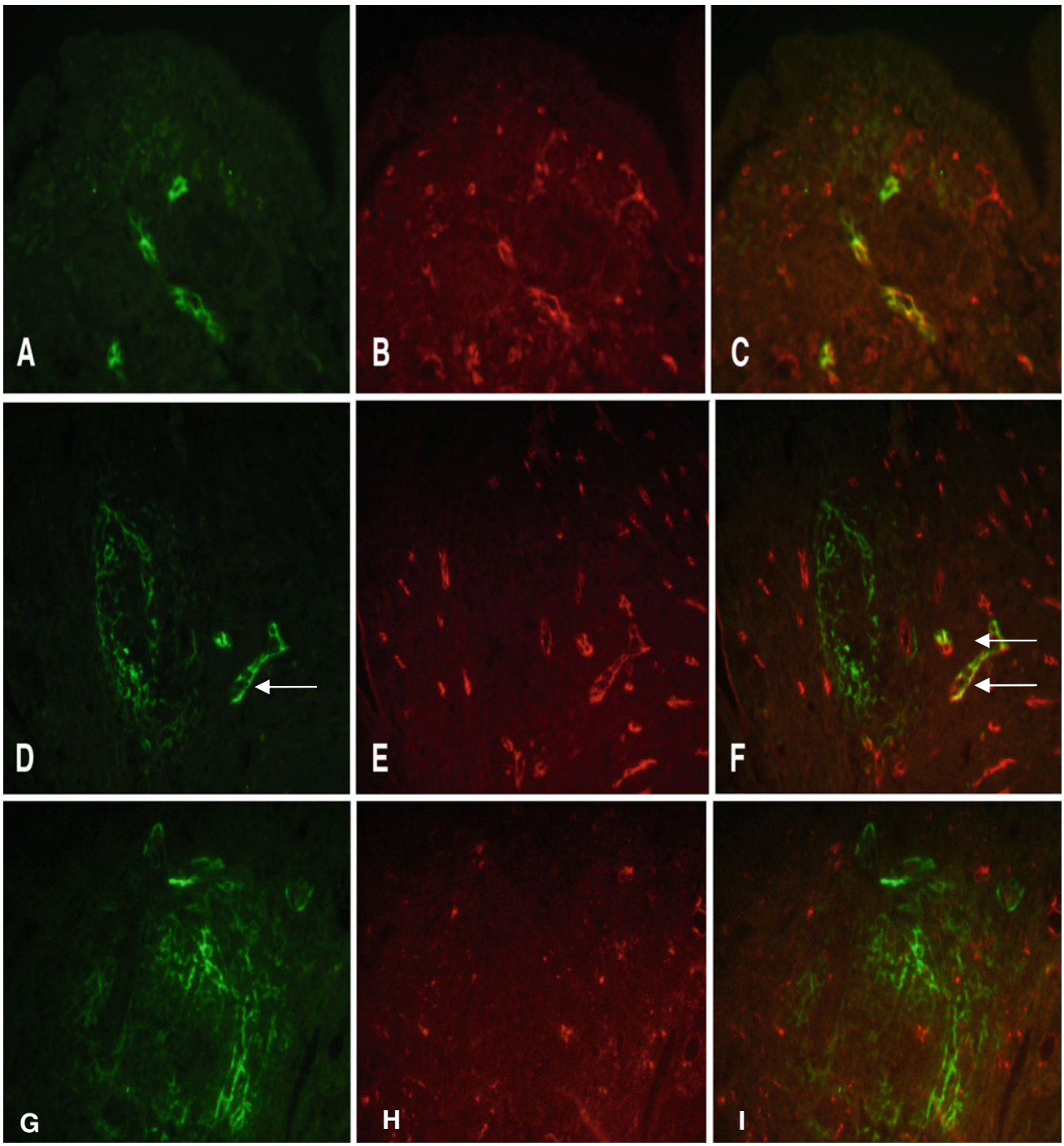

Fig. 3 **a–i** Dual immunofluorescence micrographs showing representations of MAdCAM-1 (**a** and **d** *green*), CD34 (**b** and **e** *red*) and CD 21 (**h** *red*) immunoreactivity. Panel **a** demonstrates MAdCAM-1 immunofluorescence of a peribiliary plexus around a large-sized bile duct. Panel **b** confirms the presence of CD34 immunoreactive vessels around these ducts. Panel **c** shows dual color co-localization (*yellow*) of MAdCAM-1 and CD34 fluorescence within the peribiliary plexus. Plates **d–f** show a lymphoid aggregate with a "peripheral" pattern of MAdCAM-1 immunolocalization (**d** marked with *single arrow*) which fails to co-localize with CD34 (**e**) in double staining (**f**) but colocalizes an adjacent vessel endothelium (*yellow, marked with double arrow*). Panels **g–i** show a different lymphoid aggregate from the same tissue with a "peripheral" pattern of MAdCAM-1 immunoreactivity (**g**). Focal staining was performed to exclude a dendritic cell morphology, e.g. CD21 (**h**) but did not correspond to the observed pattern of MAdCAM-1 immunoreactivity. Dual immunostaining with anti-MAdCAM-1 did not co-localize with anti-CD21 (**i**) (magnification ×20 objective)

Table 1 Semi-quantitative MAdCAM-1 staining in primary sclerosing cholangitis (PSC), primary biliary cirrhosis (PBC), hepatitis C(HCV), alcohol liver disease (ALD) related to lymphoid aggregates and peribiliary plexus

Patient	Age	Histology	Lymphoid aggregate staining pattern		Peribiliary plexus-bile duct size		
			Peripheral	Central	Large	Medium	Small
(Primary sclerosing cholangitis: n = 12) MAdCAM-1 immunostaining score							
1M	22	Cirrhosis	2+	1+	0	0	0
2F	47	Cirrhosis	2+	1+	0	1+	0
3F	28	Cirrhosis	0	0	0	2+	0
4F	35	Cirrhosis	1+	1+	0	2+	0
5M	38	Cirrhosis	0	1+	0	2+	0
6F	47	Cirrhosis	1+	1+	1+	1+	2+
7M	50	Cirrhosis	0	0	0	0	0
8M	43	Cirrhosis	3+	3+	2+	1+	1+
9M	34	Cirrhosis	0	0	0	1+	0
10M	27	Stage2	0	0	N/A	0	0
11M	35	Stage2	0	0	N/A	0	0
12M	31	Stage1	0	0	N/A	0	0
(Primary biliary cirrhosis: n = 12) MAdCAM-1 immunostaining score							
1F	61	Cirrhosis	1+	2+	0	1+	1+
2F	57	Cirrhosis	2+	3+	0	1+	1+
3F	51	Cirrhosis	1+	0	0	1+	0
4F	57	Cirrhosis	2+	0	0	1+	0
5F	36	Cirrhosis	0	1+	0	2+	0
6F	57	Cirrhosis	3+	0	0	0	0
7F	47	Cirrhosis	2+	0	0	1+	0
8F	49	Stage1	0	0	N/A	0	0
9F	52	Stage2	0	1+	N/A	0	0
10F	49	Stage2	0	0	N/A	0	0
11F	59	Stage1	0	0	N/A	0	0
12F	61	Stage1	0	0	N/A	0	0
(Hepatitis C: n = 10) MAdCAM-1 immunostaining score							
1M	51	Cirrhosis	1+	2+	0	1+	1+
2M	52	Cirrhosis	2+	1+	0	1+	0
3M	49	Cirrhosis	1+	2+	0	1+	0
4M	55	Cirrhosis	1+	0	0	1+	0
5M	48	Cirrhosis	1+	1+	0	1+	0
6M	48	Stage2	0	0	N/A	0	0
7F	54	Stage2	0	1+	N/A	0	0
8M	52	Stage2	0	0	N/A	0	0
9M	53	Stage1	0	0	N/A	0	0
10F	48	Stage1	0	0	N/A	0	0

Patient	Age	Histology	Peribiliary plexus-bile duct size		
			Large	Medium	Small
(Alcohol liver disease: n = 7) MAdCAM-1 immunostaining score					
1M	61	Cirrhosis	0	1+	0
2F	57	Cirrhosis	0	1+	0
3M	51	Cirrhosis	0	1+	0
4F	57	Cirrhosis	0	1+	0
5M	36	Cirrhosis	0	1+	1+

Table 1 continued

Patient	Age	Histology	Peribiliary plexus-bile duct size		
			Large	Medium	Small
6M	48	Cirrhosis	0	1+	0
7M	57	Cirrhosis	0	0	0

MAdCAM-1 immunostaining score

No staining 0, Light staining 1+, Moderate staining 2+, Marked staining 3+

Large ducts were not present in the needle biopsy specimens. They are classified as a N/A

the "peripheral" pattern predominates in PBC and the "central" pattern predominates in PSC, with no clear pattern apparent in HCV.

Localization of MAdCAM-1 to lymphoid aggregates was confirmed by immunofluorescence microscopy (Fig. 3d, f, g, i) as described in the methodology. Specifically, staining was performed with primary antibodies anti-human MAdCAM-1 and anti-CD34, followed by incubation with goat anti-rabbit FITC and goat anti-mouse Texas Red. Similarly, representative sections were incubated with anti-CD21, anti-CD68, anti-S100 and anti-human MAdCAM-1 primary antibodies, incubated with goat ant-rabbit FITC, goat anti-mouse Texas Red and examined by fluorescence microscopy.

Focal staining was seen with S100, CD68 and CD21 antibodies but these did not correspond to the observed pattern of MAdCAM-1 immunoreactivity. Dual immunostaining with anti-MAdCAM-1, anti-S100, CD68 and CD21 did not co-localize with MAdCAM-1. An example of this has been illustrated with CD21 in Fig. 3g–i. We explored the possibility that the "central" cells within lymphoid aggregates were CD34 positive, indicative of endothelial staining. There was focal staining evident with CD34 that matched the "central" pattern of MAdCAM-1 staining in lymphoid aggregates.

MAdCAM-1, Podoplanin and Lymphatic Endothelial Vessels (Fig. 4)

We found MAdCAM-1 did not localize to lymphatic endothelial vessels. Podoplanin was localized to vessels with morphological features of lymphatic channels that were surrounding, immediately adjacent to, and separate from lymphoid aggregates. These vessels were characterized by a single layer of flattened endothelium with intraluminal lymphocytes and without erythrocytes. They were spatially distinct from vessels expressing MAdCAM-1, including the PBP. There were occasional thin-walled branches originating from larger lymphatic vessels in porto-septal areas extending a short distance between hepatocyte plates. Co-localization of CD34 and MAdCAM-1 with a different pattern of staining than the podoplanin suggests that the vessels are capillaries of the PBP.

Real Time MAdCAM-1 Demonstrates mRNA Expression Is Relatively Higher in Cirrhosis as Compared to Normal Human Liver (Fig. 5)

We used real-time PCR to quantify levels of MAdCAM-1 mRNA per unit 18S ribosomal RNA in our liver samples. Our experiments demonstrated our ability to detect and efficiently quantify MAdCAM-1 in fresh human tissues. There were varying levels of MAdCAM-1 expression in the human liver tissues from a range of liver diseases, grouped into normal liver and cirrhotic liver explants. There was significant upregulation of MAdCAM-1 expression in the cirrhotic liver ($p < 0.011$) as compared to normal liver, consistent with our histological findings.

MAdCAM-1 Is Constitutively Expressed in Normal Human Liver and Colon

Sequence analysis of cDNA of MAdCAM-1 from normal liver (Fig. 6) shows electrophoretogram/sequence of human *MAdCAM-1* using specific PCR primer sequences and amplified cDNA transcribed from RNA extracted from histologically normal liver, indicating consensus between sequenced material and MAdCAM-1 sequence information from GenBank, i.e. presence of constitutive MAdCAM-1 in normal liver. The identical sequence was also extracted from colon.

Discussion

This study demonstrates significant up-regulation of MAdCAM-1 expression in cirrhosis and its notable absence in normal and pre-cirrhosis. Specifically, we found MAdCAM-1 to be localised to septal areas primarily within: (1) endothelium of the PBP and (2) intra-hepatic

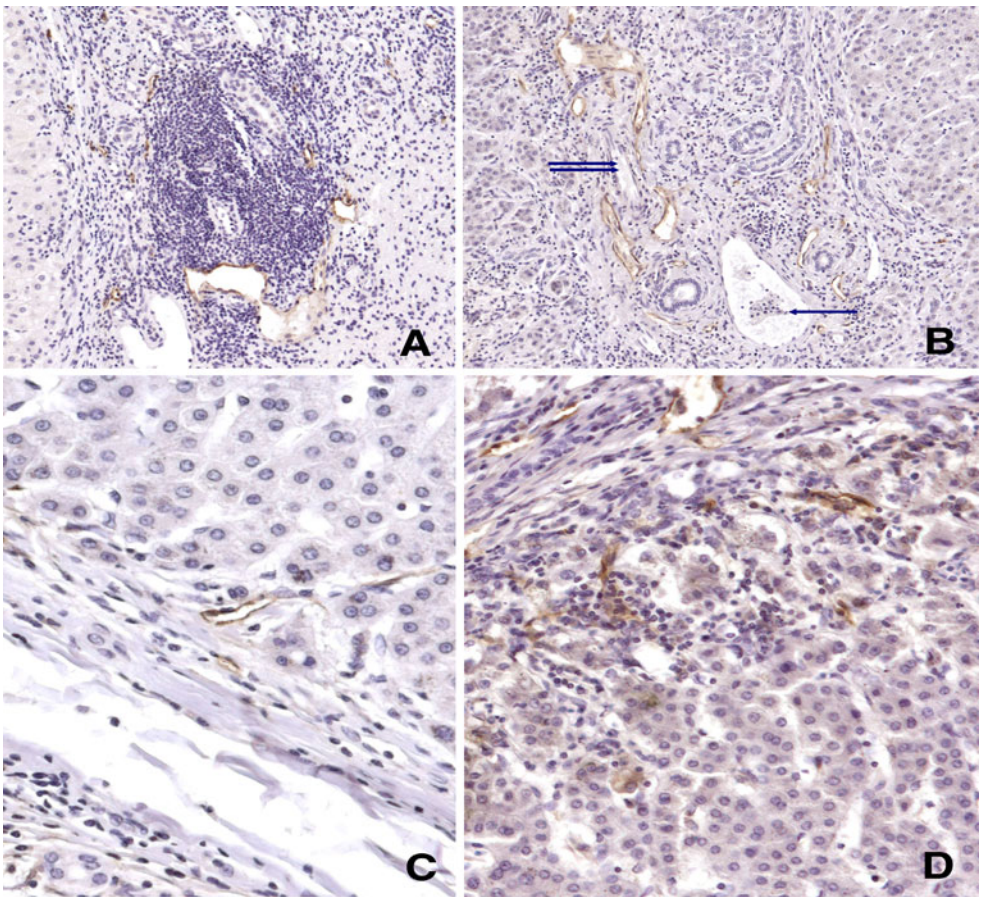

Fig. 4 **a**–**d** Immunohistochemical localization of the lymphatic phenotypic marker podoplanin in PSC and PBC. Plates **a** and **b** demonstrate podoplanin staining patterns of vessels around a lymphoid aggregate, but not conforming to "peripheral" or "central" MAdCAM-1 immunoreactivity. Note the portal vein (*single arrow*) containing red blood cells is identifiable, as is the muscular wall of the hepatic artery (*double arrow*), and neither shows podoplanin immunoreactivity. Plates **c** and **d** show podoplanin staining into lymphatic channels, which extend a short distance into the parenchyma from porto-septal areas, both in the presence and absence of inflammatory cells. (Alkaline phosphatase immunostaining: magnification ×10 objective **a**, **b**, ×20 objective **c**, **d**)

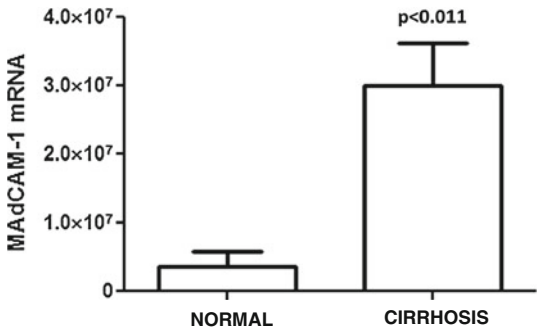

Fig. 5 Expression of MAdCAM-1 mRNA in the human liver as determined by real-time PCR

lymphoid aggregates. We confirmed the presence of MAdCAM-1 expression in liver disease characterised by portal inflammation, e.g. PSC and PBC, and extended these observations to show its presence in other chronic liver diseases which are more associated with lobular inflammation, such as ALD, as well as those which are unrelated to gastrointestinal inflammation, such as HCV.

The PBP are a network of delicate small vessels surrounding the intrahepatic bile ducts supplied by branches of the hepatic artery, which drain into hepatic sinusoids or branches of the portal vein [14]. The PBP is the main vascular supply of the biliary epithelium. It functions in supporting the secretory and absorptive properties of the biliary epithelium. We found MAdCAM-1 to be expressed in the PBP predominantly in medium bile duct sizes in PSC and PBC explants. The specificity of MAdCAM-1 immunoreactivity is indicated by the fact that bile ducts are not stained. The vascular endothelial nature of these structures was confirmed by dual immunofluorescence with MAdCAM-1 and CD34. The distribution of MAdCAM-1 around the bile ducts differed between PSC and PBC. The smaller single capillary layer ducts showed similar levels in both conditions, but only large-sized bile ducts (i.e. greater than 100 μm in diameter, usually septal or trabecular ducts)

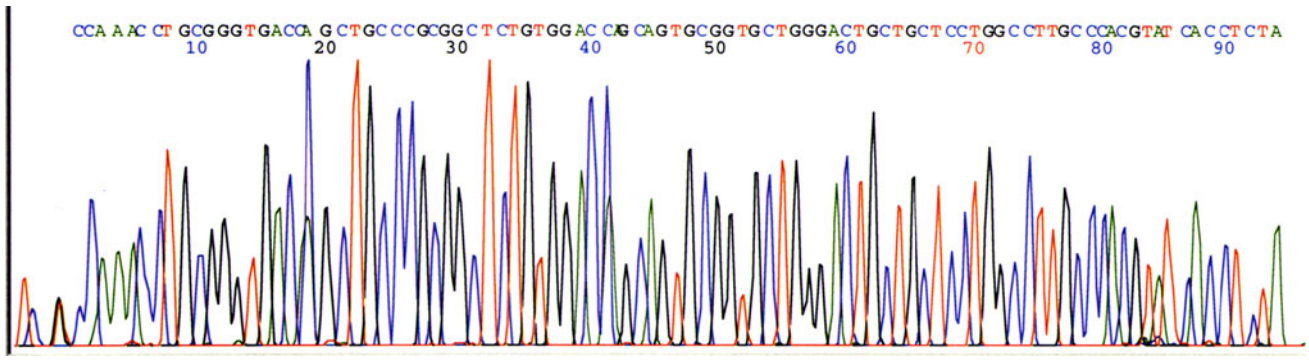

Fig. 6 Electrophoretogram and sequence of human MAdCAM-1 using specific PCR primer sequences and amplified cDNA transcribed from RNA extracted from histologically normal liver, indicating consensus between sequenced material and MAdCAM-1 sequence information from GenBank, i.e. presence of constitutive MAdCAM-1 in normal liver. The identical sequence was also extracted from colon

expressed MAdCAM-1 only in PSC and where its immunoreactivity is noteworthy in comparison to PBC and HCV. This observation is particularly interesting, since PSC involves larger ducts than PBC. That is, the absence of large duct inflammation in PBC and lack of MAdCAM-1 expression around these ducts may reflect regional distribution of disease, which is further supported by MAdCAM-1 staining around its small bile ducts. The vessels of the PBP may represent transformed high-endothelial venules which in other sites are well characterised for their role in leukocyte trafficking [15, 16].

There is little evidence thus far on the expression of vascular adhesion molecules on the PBP. Yasoshima et al. [17] showed these vessels to express ICAM-1 in PBC but did not study MAdCAM-1. The vascular endothelium can secrete pro-inflammatory cytokines, e.g. TNFα, and this is a likely amplification step leading to the upregulation of adhesion molecules on the endothelium of the PBP [18]. The presence of MAdCAM-1 on the endothelium of the PBP is presumptive of a role in lymphocyte emigration and recruitment, suggesting MAdCAM-1 acts as a local addressin at these sites, using the endothelium of the PBP for egress and as a recirculatory pathway to areas of inflammation such as those around bile ducts. The possibility that this egress occurs in capillaries is intriguing because this lymphocyte-endothelium interaction could occur in low velocity flow states. The functional significance of the expression of MAdCAM-1 on the PBP is uncertain, as they are also present in cases of HCV and ALD cirrhosis, where bile duct injury is not a major feature. It is possible that the structures immunoreactive to MAdCAM-1 on the PBP are functionally post-capillary sinuses which are ideal sites for lymphocyte egress.

Whether MAdCAM-1 upregulation is in fact a late event in the pathogenesis of chronic liver disease or a secondary epiphenomena type response to inflammation is not known. Cholestasis alone is unlikely to be responsible for MAdCAM-1 upregulation due to our lack of expression in extrahepatic obstruction. In PBC, other adhesion molecules such as ICAM-1 appear to be expressed commensurate with the level of inflammation [19]. Interestingly, from our immunohistochemistry work we found no evidence of MAdCAM-1 expression in pre-cirrhosis (PBC, PSC, HCV). In contrast, we detected MAdCAM-1 in nearly all cirrhotic liver and the distinct absence in the non-cirrhotic liver (non-cirrhotic portal hypertension, pre-cirrhosis and normal liver). It therefore follows that the upregulation of MAdCAM-1 was unlikely to be due to the effects of portal hypertension.

The observation that the majority of MAdCAM-1 was upregulated on cirrhotic liver suggests that its upregulation might be related to the fibrogenesis or neovascularization of cirrhosis. Certainly, TNFα activation of fibroblasts reportedly induces expression of MAdCAM-1 [20]. The possibility that some of the endothelium-lined vessels showing immunoreactivity to MAdCAM-1 were actually lymphatic in origin was considered using the endothelial cell-surface glycoprotein podoplanin [21]. We demonstrated podoplanin expression on vessels with morphological features of lymphatic vasculature, subjacent to and separate from lymphoid aggregates, and these each were morphologically distinct from vessels expressing MAdCAM-1.

There appeared two populations of MAdCAM-1 positive cells in the lymphoid aggregates. We have described the pattern of MAdCAM-1 expression in lymphoid aggregates as “peripheral” or “central” with immunoreactivity in vessel endothelium likely to be the HEV. Although definitive conclusions could not be made from our experiments regarding the nature of the “peripheral” staining pattern, they may represent MAdCAM-1 expression on the specialised dendritic cells, e.g. interdigitating reticular cells, FDC or macrophages [22]. We explored the possibility that the cells within lymphoid aggregates were CD34 positive. There was focal staining evident with CD34 that matched the “central” pattern of MAdCAM-1 staining in lymphoid

aggregates. Dual immunostaining with MAdCAM-1 and CD34 to extend these experiments would have been useful to confirm whether these cells were vascular endothelial in origin, e.g. HEV. The inflammatory processes within the liver may up-regulate MAdCAM-1 locally, enhancing recruitment of antigen specific cells. Although there was focal staining seen with S100, CD68 and CD21 antibodies, surprisingly this did not correspond to the pattern seen for MAdCAM-1. Dual immunostaining was also performed with anti-MAdCAM-1 and anti-S100, CD68, and CD21 but these did not co-localise with MAdCAM-1. Our results appear to suggest that the "peripheral" pattern predominates in PBC cirrhosis and the "central" pattern predominates in PSC cirrhosis, with no clear pattern emerging in end stage HCV and absence of lymphoid aggregates in ALD. From these observations, it is tempting to correlate the lymphoid patterns to pathogenesis of disease. Certainly, the morphology of the "peripheral" lymphoid MAdCAM-1 staining pattern appeared similar to dendritic cells, e.g. FDC, present in Peyer's patch, resembling VCAM-1 and ICAM-1 immunoreactivity in lymphoid aggregates from end-stage viral hepatitis, e.g. HCV [16], through which they can support antigen presentation to $\alpha4\beta1$ and LFA-1 expressing B cells, respectively, in germinal centres, thus leading to their maturation and differentiation into memory cells. Hepatic expression of MAdCAM-1 on dendritic cells could serve as a signal for retention of $\alpha4\beta7$ lymphocytes in the liver. The possibility of HEV within lymphoid aggregates raises the further possibility of its importance in lymphocyte egress and effective recirculation to areas of inflammation. Unfortunately, the dendritic cell markers used in our study did not appear to give any comparable immunoreactivity. Certainly more extensive dual staining using specific markers for further dendritic cell subsets is required to define exactly where MAdCAM-1 protein is expressed. If MAdCAM-1 appears to be expressed in dendritic cells within the liver then this would suggest that it has a more extensive role then acting as an addressin in chronic liver disease.

The activation of $\alpha4\beta7$ mucosal lymphocytes recruited from the gut to the PSC liver is a possible mechanism by which hepatic inflammation is maintained in some patients with IBD. The concept that lymphocytes programmed to home to the gut may also home to the liver constitutes an attractive hypothesis linking chronic IBD with liver inflammation. These results concur with those by Grant et al. confirming MAdCAM-1 expression in liver cirrhosis secondary to PSC [12, 23, 24]. We have extended these observations to demonstrate MAdCAM-1 in other cirrhotic liver diseases such as PBC (where we see similar patterns of MAdCAM-1 expression in the vascular beds of the PBP) as well as ALD and HCV. We did not see MAdCAM-1 expression in normal liver, extrahepatic biliary obstruction nor pre-cirrhotic stages of other liver diseases (e.g. HCV, PBC, ALD). In all cases, the isotype-matched control used displayed no reactivity, suggesting that the stain with anti-MAdCAM-1 was real.

A distinct and important observation from our real-time experiments is that MAdCAM-1 is present constitutively in normal human liver, albeit only in relatively small quantities, where it probably exists with a divergent structural folding. This could explain the relatively low expression levels of MAdCAM-1 in some immunohistochemical studies (Grant et al. using monoclonal antibodies) and absence in others, such as ours using polyclonal antibodies [12, 24]. Currently, the epitope where the monoclonal antibody binds is not known. It acts as a function-blocking antibody and it is likely that it recognizes an epitope in either of the two extracellular domains. In the normal liver setting, the non-functional folded state cannot support lymphocyte recruitment, whereas in inflammatory conditions the local release of TNFα could induce further expression of MAdCAM-1. It is possible that stimulatory agents, e.g. chemokines, in combination with the already expressed MAdCAM-1 acquires a functional confirmation, thus being allowed to recognize leukocyte-integrin recognition and binding [25]. There would certainly be merit in exploring this further.

Using real-time analysis (qPCR), we have shown the significant upregulation of MAdCAM-1 mRNA (Fig. 5) in cirrhosis ($p < 0.011$) compared to normal liver, confirming the findings from our immunohistochemical analysis and refuting the suggestion of an epiphenomena from cirrhosis. Sequence analysis of cDNA from a normal liver (Fig. 6) revealed complete alignment with the MAdCAM-1 gene sequence, thus validating the presence of MAdCAM-1, albeit in relatively small quantities. Blocking MAdCAM-1 might specifically reduce hepatic inflammation in the cirrhotic liver without widespread immunosuppression that would be of therapeutic benefit.

We conclude that hepatic MAdCAM-1 is upregulated in cirrhosis, regardless of the underlying liver disease. The expression of MAdCAM-1 is localized to PBP and lymphoid aggregates in cirrhosis and may contribute to the localization and recruitment of $\alpha4\beta7$ lymphocytes during the pathogenesis of these conditions. Our study demonstrates our ability to detect and effectively quantify MAdCAM-1 in human liver. MAdCAM-1 could be a surrogate marker of advanced liver disease with pathological and morphological value in evaluating chronicity. Equally, its absence could have prognostic value in pre-cirrhosis. Further studies to evaluate and dissect its expression in advanced liver disease within the presence of reversible and non-reversible stages could be worthy of future support.

Acknowledgments A. A. was supported by a Wellcome Trust Training Fellowship, Royal College of Physicians London Sheila

Sherlock Hepatology Travelling Fellowship, St Johns Ambulance Trust, Digestive Diseases Foundation/Tana Trust Project grants and the National Institute of Health and Research (NIHR). The work was approved by The Royal Free Hospital Ethics Committee (Ethics ID 5441, Project ID 5441). We are grateful to Dr Kerjaschki, Dept of Clinical Pathology, University of Vienna for the gift of antipodoplanin antibody.

Conflict of interest None.

References

1. Butcher EC. Leukocyte-endothelial cell recognition: three (or more) steps to specificity and diversity. *Cell*. 1991;67:1033–1036.
2. Briskin MJ, Rott L, Butcher EC. Structural requirements for mucosal vascular addressin binding to its lymphocyte receptor alpha 4 beta 7. Common themes among integrin-Ig family interactions. *J Immunol*. 1996;156:719–726.
3. Berg EL, McEvoy LM, Berlin C, Bargatze RF, Butcher EC. L-selectin-mediated lymphocyte rolling on MAdCAM-1. *Nature*. 1993;366:695–698.
4. Wagner N, Lohler J, Kunkel EJ, et al. Critical role for beta7 integrins in formation of the gut-associated lymphoid tissue. *Nature*. 1996;382:366–370.
5. van der Feltz MJ, de Groot N, Bayley JP, Lee SH, Verbeet MP, de Boer HA. Lymphocyte homing and Ig secretion in the murine mammary gland. *Scand J Immunol*. 2001;54:292–300.
6. Briskin M, Winsor-Hines D, Shyjan A, Cochran N, et al. Human mucosal addressin cell adhesion molecule-1 is preferentially expressed in intestinal tract and associated lymphoid tissue. *Am J Pathol*. 1997;151:97–110.
7. Schweighoffer T, Tanaka Y, Tidswell M, Erle DJ, et al. Selective expression of integrin alpha 4 beta 7 on a subset of human CD4+ memory T cells with Hallmarks of gut-trophism. *Immunology*. 1993;151:717–729.
8. Souza HS, Elia CC, Spencer J, MacDonald TT. Expression of lymphocyte-endothelial receptor-ligand pairs, alpha4beta7/MAdCAM-1 and OX40/OX40 ligand in the colon and jejunum of patients with inflammatory bowel disease. *Gut*. 1999;45:856–863.
9. Hokari R, Kato S, Matsuzaki K, Iwai A, et al. Involvement of mucosal addressin cell adhesion molecule-1 (MAdCAM-1) in the pathogenesis of granulomatous colitis in rats. *Clin Exp Immunol*. 2001;126:259–265.
10. Kato S, Hokari R, Matsuzaki K, Iwai A, et al. Amelioration of murine experimental colitis by inhibition of mucosal addressin cell adhesion molecule-1. *J Pharmacol Exp Ther*. 2000;295:183–189.
11. Hillan KJ, Hagler KE, MacSween RN, Ryan AM, et al. Expression of mucosal vascular addressin MAdCAM, in inflammatory liver disease. *Liver*. 1999;19:509–518.
12. Grant AJ, Lalor PF, Hubscher SG, Briskin M, Adams DH. MAdCAM-1 expressed in chronic inflammatory liver disease supports mucosal lymphocyte adhesion to hepatic endothelium (MAdCAM-1 in chronic inflammatory liver disease). *Hepatology*. 2001;33:1065–1072.
13. Lefkowitch J. *Scheuer's Liver Biopsy Interpretation*. Saunders (W.B.) Co Ltd; 2010.
14. Kobatashi S, Nakanuma Y, Matsui O. Intrahepatic peribiliary vascular plexus in various hepatobiliary diseases: a histological survey. *Hum Pathol*. 1994;25:940–946.
15. Girard JP, Springer TA. High endothelial venules (HEVs): specialised endothelium for lymphocyte migration. *Immunol Today*. 1995;16:449–457.
16. Garcia-Monzon C, Sanchez-Madrid F, Garcia-Buey L, Garcia-Arroyo A, Garcia-Sanchez A, Moreno-Otero R. Vascular adhesion molecule expression in viral chronic hepatitis: evidence of neoangiogenesis in portal tracts. *Gastroenterology*. 1995;108:231–241.
17. Yasoshima M, Nakanuma Y, Tsuneyama K, Van de Water J, Gershwin ME. Immunohistochemical analysis of molecules in the micro-environment of portal tracts in relation to aberrant expression of PDC-E2 and HLA-DR on the bile ducts in primary biliary cirrhosis. *J Pathol*. 1995;175:319–325.
18. Denk A, Goebeler M, Schmid S, et al. Activation of NF-kappa B via IkappaB kinase complex is both essential and sufficient for proinflammatory gene expression in primary endothelial cell. *J Biol Chem*. 2001;276:28451–28458.
19. Adams DH, Hubscher SG, Shaw J, et al. Increased expression of intracellular adhesion molecule-1 on bile ducts in primary biliary cirrhosis and primary sclerosing cholangitis. *Hepatology*. 1991;14:426–431.
20. Oshima T, Pavlick KP, Laroux FS, Verma SK, et al. Regulation and distribution of MAdCAM-1 in endothelial cells in vitro. *Am J Physiol Cell Physiol*. 2001;281:C1096–C1105.
21. Breiteneder-Geleff S, Matsui K, Soleiman A, Meraner P, et al. Podoplanin, novel 43-kd membrane protein of glomerular epithelial cells, is down-regulated in puromycin nephrosis. *Am J Pathol*. 1997;151:1141–1152.
22. Szabo MC, Butcher EC, McEvoy LM. Specialisation of mucosal follicular dendritic cells revealed by mucosal addressin-cell adhesion molecule-1 display. *J Immunol*. 1997;158:5584–5588.
23. Grant AJ, Lalor PF, Salmi M, Jalkanen S, Adams DH. Homing of mucosal lymphocytes to the liver in the pathogenesis of hepatic complications of inflammatory bowel disease. *Lancet*. 2002;359:150–157.
24. Liaskou E, Karikoski M, Reynolds GM, Lalor PF, Weston CJ, et al. Regulation of mucosal addressin cell adhesion molecule 1 expression in human and mice by vascular adhesion protein 1 amine oxidase activity. *Hepatology*. 2011;53:661–672.
25. Miles A, Liaskou E, Eksteen B, Lalor PF, Adams DH. CCL25 and CCL28 promote alpha4 beta7-integrin-dependent adhesion of lymphocytes to MAdCAM-1 under shear flow. *Am J Physiol Gastrointest Liver Physiol*. 2008;294:G1257–G1267.